Dissociative Double Ionization of CO_2: Dynamics, Energy Levels, and Lifetime†

Vandana Sharma,‡ B. Bapat,‡ Jagannath Mondal,§,# M. Hochlaf,⊥ Kousik Giri,§ and N. Sathyamurthy*,§

Physical Research Laboratory, Ahmedabad 380 009, India, Department of Chemistry, Indian Institute of Technology Kanpur, Kanpur 208 016, India, and Theoretical Chemistry Group, Université de Marne-la-Vallée, F-77454 Marne la Valleé, France

Received: January 12, 2007; In Final Form: March 21, 2007

In a kinematically complete experiment on the dissociative double ionization of CO_2 by electron impact, spontaneous and metastable decay have been observed via the channel $CO_2^{2+} \rightarrow CO^+ + O^+$. The metastable decay shows a lifetime of 5.8 ± 1.5 μs. The measured kinetic energy release spectrum of the dissociation shows one broad peak. To understand the observed features, ab initio potential energy surface (PES) for the ground electronic state of CO_2^{2+} was computed using a multireference configuration interaction method and a correlation-consistent polarized-valence quadruple-ζ basis set, for a range of internuclear distances and O−C−O bond angles, and an analytic fit of the PES was obtained. The computed PES clearly indicates the metastability of the dication and yields a barrier height and an asymptotic limit in fair agreement with the reported data. A time-dependent quantum mechanical approach was used to compute the ground vibrational state wave function of CO_2 in its ground electronic state. Assuming a Franck−Condon transition, the same function was taken to be the initial wave function at time $t = 0$ for the time evolution on the fitted PES for the ground electronic state of CO_2^{2+}. The autocorrelation function was computed and Fourier transformed to obtain the excitation spectrum. Upon convolution with the instrument resolution function, the kinetic energy release spectrum was obtained, in good agreement with the experimental results, particularly at lower energies. The discrepancies at higher energies are attributed to the noninclusion of the excited states of CO_2^{2+} in the dynamical study.

I. Introduction

The CO_2^{2+} dication has frequently been studied experimentally since it was first observed in 1964.[1] Various methods such as photoionization, electron impact ionization, charge transfer, single-electron capture, Auger spectroscopy, and charge separation mass spectrometry have been designed to study the appearance energy, the excitation energies of higher electronic states, dissociation thresholds, charge separation branching ratios, and lifetimes.[2−4] The instability of most molecular ions with charges greater than or equal to 2 precludes experimental study of their structure by traditional spectroscopic techniques. Fragment detection and kinetic energy spectroscopy are necessary. A more elaborate method is fragment momentum spectroscopy, which has emerged as the method of choice in the past decade. Theoretical prediction of the instability is a challenge because most strategies for determining the potential energy surface (PES) depend on variational techniques.

The dication of CO_2 was first studied theoretically using the one-electron approximation, self-consistent field (SCF), and restricted configuration interaction (CI) methods for the purpose of calculating the Auger transition intensities and energies.[5] Subsequently, the vertical excitation spectrum was computed[3] by ab initio SCF-CI calculations. But these computations were restricted to the equilibrium geometry of CO_2, and there was no information available on the PES of CO_2^{2+} until Hogreve[6] showed that the ground-state PES of CO_2^{2+} had a local minimum for the collinear symmetric configuration. Unfortunately, his study was restricted to the collinear geometry. Hochlaf et al.[7] extended the study to three dimensions with the main aim of providing insight into the shape of the PES for the electronic ground state of CO_2^{2+} and to deduce its spectrum. The resulting spectral assignment has been published elsewhere.[8] Much of their work was confined to energies up to only 8000−12 000 cm^{-1} above the minimum and *not* to the region leading to the dissociation of the dication. Therefore, it was decided to extend the ab initio calculations further to geometries leading to $CO^+ + O^+$ in three dimensions. In view of the good agreement between the predicted and the observed spectra in the earlier study, the additional calculations were carried out at the same level of theory used previously, that is, spdf cc-pVQZ/MRCI.

For the purpose of subsequent dynamical studies, an analytic function was fitted to the ab initio PES, and the dissociative dynamics of CO_2^{2+} was investigated using a time-dependent quantum mechanical wave packet approach.[9] Krishnamurthy et al.[10] demonstrated the utility of such an approach to the dissociation dynamics of diatomic cations. More recently, Tarisien et al.[11] showed how the approach could account for the experimentally observed kinetic energy release (KER) spectrum of CO^{2+}. The method makes use of the fact that the target molecule CO_2 undergoes multiple ionization due to the impact of the fast moving electron in a Franck−Condon manner. What this means is that the stationary state wave function

† Part of the special issue "Robert E. Wyatt Festschrift"

* To whom correspondence should be addressed. E-mail: nsath@iitk.ac.in.
‡ Physical Research Laboratory.
§ Indian Institute of Technology Kanpur.
⊥ Université de Marne-la-Vallée.
Present address: Department of Chemistry, University of Wisconsin, Madison, WI 53706.

10.1021/jp070257k CCC: $37.00
Published on Web 05/11/2007

$|\Psi_g^{CO_2}(0,0,0)\rangle$ for the ground vibrational state of the CO_2 molecule in its ground electronic state becomes the nonstationary state wave function $|\Psi_g^{CO_2{}^{2+}}(t=0)\rangle$ for the newly created dicationic state, and it evolves with time on the PES for the ground electronic state of CO_2^{2+}:

$$|\Psi_g^{CO_2}(0,0,0) \rightarrow |\Psi_g^{CO_2{}^{2+}}(t=0) \xrightarrow{H_g^{CO_2{}^{2+}}} |\Psi(t)$$

Here, $H_g^{CO_2{}^{2+}}$ represents the Hamiltonian for the ground electronic state of CO_2^{2+}. The autocorrelation function $c(t) = \langle\Psi(t=0)|\Psi(t)\rangle$ for the ground state of CO_2^{2+} is Fourier transformed to yield the power spectrum, which, when convoluted with the instrument resolution function, yields the KER spectrum that could be compared with the experimentally measured spectrum. Although there are several other dissociative channels (such as $C^+ + O_2^+$) opening up at higher energies, the present study focuses on the lowest energy and the most important channel, $CO^+ + O^+$. Experimental methods and the results are presented in Section II. The details of the calculations of the ab initio PES, the determination of the ground-state eigenfunction for CO_2, the time evolution of the wave function on the ground electronic state of CO_2^{2+}, and the computation of the KER spectrum are described in Section III. A summary and conclusion follow in Section IV.

II. Experiment

A. Apparatus and Data Acquisition. The experiment is performed using an ion momentum spectrometer that has been described elsewhere.[12] Other methods, such as velocity map imaging (VMI) and several variants of time-of-flight spectrometry with imaging detectors, are used for momentum resolved measurements. However, a single-field time-of-flight spectrometer with position-sensitive detection has an advantage over VMI, primarily because there is no need to time-slice the events for inverting the spatial and temporal dispersion data into momentum distributions. The spectrometer can be regarded as a time-of-flight spectrometer with a large area position-sensitive detector, permitting simultaneous recording of the instant and position of arrival of ions. Ions are formed by collisions between electrons with energies of 1300 eV and CO_2 molecules from an effusive beam in a crossed-beams arrangement. The overlap volume is about 2 mm^3. Ions are extracted by a homogeneous electric field with a strength of 30 V/cm or 60 V/cm and are identified by their time of flight. The same electric field forces the ejected electrons in the opposite direction to another detector. Suitably placed and biased electrodes guide the projectile electrons to a Faraday cup, while preventing them from reaching the ejected electron detector. Ejected electron detection provides the start trigger for ion time-of-flight measurement. The time lapse between electron detection and the instant of ionization is negligible compared to the ion flight time. The arrival of the ion on the detector stops the flight time measurement. Using the same start trigger, up to four ions from a single ionization event (called hits) can be separated on the basis of their flight times. Flight-time measurement and the position information for each hit is stored event after event in a list. The flight time and position of each ion hit can be related to the initial momentum of the ion in an analysis performed after the experiment is over. By applying suitable conditions to the event list data, one obtains the momentum vectors of all ions, from which various quantities such as the angle of emission, kinetic energy, and so forth can be derived. For ion pairs formed by the dissociation of doubly ionized molecules, the subset of the event list having two hits is sorted out. This subset is then plotted as a $(t_1{:}t_2)$ coincidence map, which shows the correlated flight times of ion pairs arising from a single event. In the present case of dissociation of CO_2^{2+}, which can result into, at most, three fragments with $3N - 4$ phase space degrees of freedom, complete details of the dissociation can be obtained via 5-fold correlation maps. The $(t_1{:}t_2)$ coincidence map for the present collision system obtained with an extraction field of 30 V/cm is shown in Figure 1.

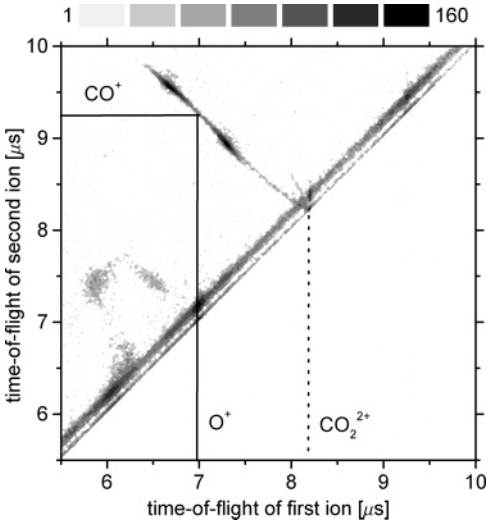

Figure 1. Ion pair coincidence map of fragments arising from the dissociation of CO_2^{2+}. The prominent feature along the reverse diagonal is the distribution of the correlated flight times of O^+ and CO^+. The less intense islands in the lower left portion of the plot are due to other dissociation products $C^+ + O^+ + O$ and $C + O^+ + O^+$. The tail and the V emerging from the main $CO^+{:}O^+$ distribution are due to metastable states, as explained in the text. The t_1 ordinate of the dotted line is the flight time of CO_2^{2+}, if it were to remain intact.

B. Dissociation Channels, Metastability, and Kinetic Energy. Three prominent islands are seen in the coincidence map, corresponding to the channels $CO_2^{2+} \rightarrow O^+ + CO^+$, $C^+ + O^+ + O$, and $C + O^+ + O^+$. Of special interest is the dominant two-body dissociation channel leading to the coincident ion pair $CO^+{:}O^+$. The $CO^+{:}O^+$ coincidence counts are mainly distributed as an island along the reverse diagonal in the $t_1{:}t_2$ coincidence map. The main island is due to prompt dissociation. There are two additional features associated with this island, which are indicative of a metastable decay. The first is a long tail extending to the forward diagonal of the plot. The second (weaker) feature is V-shaped scatter at the end of the tail and close to the forward diagonal. The flight times of the O^+ and CO^+ ions would be correlated irrespective of the type of decay, but in the case of metastable decay, the dissociating CO_2^{2+} ion travels some distance along the extraction field before dissociating. This results in a shift in the flight times, of both O^+ and CO^+, from their values in the case of prompt dissociation. If the lifetime of the dication is significantly longer than the time spent by the ion in the accelerating region, there will be break-ups occurring in the field-free region of the time-of-flight spectrometer. The latter gives rise to the V. The lifetime (assuming a single component) can be obtained from the counts in the V (I_V) and in the tail (I_{tail}) and the flight time of the dication through the acceleration and drift regions, if it is stable.[14] For a single-field time-of-flight spectrometer, the acceleration and drift times are equal. If the total flight time is T, and f is the transmission factor of the spectrometer, then the lifetime τ is obtained from the relationship

$$\frac{I_{\text{tail}}}{I_{\text{V}}} = f \exp(T/2\tau) \quad (1)$$

From the spectra recorded at 30 V/cm, the lifetime was obtained as $5.8 \pm 1.5\ \mu$s. The transmission factor is defined as the product of the geometrical transmission factors of the two meshes in the spectrometer (0.95 each). Furthermore, it has been verified by computer simulation of the trajectories of CO^+ and O^+ ions that their transmission through the spectrometer (assuming perfect meshes) is 100% if their kinetic energy is less than 10 eV. In the simulation, ions are assumed to arise from a source with a volume of 1 mm^3 and are assumed to be emitted isotropically. The maximum kinetic energy (as determined from the axial momentum is 10 eV.[13]

Several lifetimes of this dication ranging from 0.9−21.6 μs have been reported in the past.[14−16] The reported values are approximately correlated with the value of T. This suggests that there are indeed several metastable decays, and the one most likely to be well sampled depends on the apparatus. In the coincidence spectrum obtained at 60 V/cm extraction, the intensity in the V cannot be determined, as the arms of the V are very short and overlap with the false coincidences along the diagonal.

Kinetic energies of the coincident CO^+ and O^+ ions are determined for each event. The sum of the kinetic energies is histogrammed, giving the KER spectrum. To prevent a bias against high kinetic energy ions, kinetic energy analysis is done for data obtained with a high extraction field (60 V/cm). The experimental spectrum is compared with the theoretical prediction, after convolving the prediction with the instrumental width of 170 meV (see below). The experimental KER distribution appears to have two merged peaks, suggesting contributions from two electronically excited states.

III. Theory

A. Potential Energy Surface. The ground-state PES for neutral CO_2 was taken from the work of Hochlaf et al.[7] The ground-state PES of CO_2^{2+} was generated using the multireference configuration interaction (MRCI) method, with the correlation-consistent polarized-valence quadruple-ζ (cc-pVQZ) basis set with the help of the MOLPRO[17] suite of programs on a grid of points with C−O bond lengths r_1, r_2 ranging from $1.8a_0$ to $5.5a_0$ and an O−C−O bond angle of $\theta = 90°$ (45°) 180°. Since the geometry of the dication is collinear in its equilibrium state, the molecule gets highly strained when the bond angle becomes less than 90°. As a result, the computation of ab initio points becomes difficult for bond angles less than 90° due to a convergence problem. So, our PES calculations were restricted to O−C−O bond angles in the range of $\theta = 90-180°$.

An analytic functional fit to the computed ab initio potential energy values was obtained using the many-body expansion method of Aguado et al.[18] The potential energy function for a triatomic system *ABC* (A = O, B = C, C = O) is written as

$$V_{ABC}(R_{AB},R_{BC},R_{AC}) = V_A^{(1)} + V_B^{(1)} + V_C^{(1)} + V_{AB}^{(2)}(R_{AB}) + V_{BC}^{(2)}(R_{BC}) + V_{AC}^{(2)}(R_{AC}) + V_{ABC}^{(3)}(R_{AB}, R_{BC}, R_{AC}) \quad (2)$$

The diatomic potential for *AB* is given by

$$V_{AB}^{(2)} = \frac{c_0 \cdot \exp(-\alpha_{AB} \cdot R_{AB})}{R_{AB}} + \sum_{i=1}^{L} c_i \rho_{AB}^i \quad (3)$$

where $L = 5$ for CO^+ and 7 for O_2^+. The Rydberg-type variables ρ are given by

$$\rho_{AB} = R_{AB} \cdot \exp(-\beta_{AB}^l \cdot R_{AB}),\ l = 2 \text{ (two-body) or } 3 \text{ (three-body)} \quad (4)$$

Similar expressions hold for *BC* and *CA*.

The linear parameters c_i; $i = 0$ ... N and the nonlinear parameters α_{AB} and β_{AB}^2 were determined by fitting to the ab initio values corresponding to the ground-state of the diatomic fragments (plus a separated atom at a large enough distance) computed with the same basis set used for the triatomic system and using the same ab initio procedure. The three-body term $V_{ABC}^{(3)}$ is written as

$$V_{ABC}^{(3)}(R_{AB}, R_{BC}, R_{AC}) = \sum_{ijk}^{M} d_{ijk} \rho_{AB}^i \rho_{BC}^j \rho_{AC}^k \quad (5)$$

The indices i, j, and k vary from zero to a maximum value such that

$$i + j + k \neq i \neq j \neq k \quad (6)$$

$$i + j + k \leq M \quad (7)$$

A total of 969 calculated MRCI points have been used for the fit that uses $M = 6$. The energy of the three separated atoms in their ground electronic states has been taken to be the zero of energy. Compared to the computed ab initio potential energy values, the fitted surface has a root-mean-square deviation of 0.294 eV.

Parameters resulting from the analytic fit are listed in Table 1. The FORTRAN subroutine describing the PES is available upon request. Potential energy contours in (r_1, r_2) space for $\theta = 90°$, 135°, and 180° are illustrated in Figure 2 along with the cross sections, with one of the distances fixed at $r_{CO} = r_1^e$ for the collinear geometry, for different values of θ. A comparison of the fitted data with the reported characteristics of the PES is given in Table 2. It can be seen that the fitted energy of the local minimum of the dication and its equilibrium bond lengths are in excellent agreement with the data reported by Hochlaf et al.[7] The barrier height (2.0 eV) for dissociation CO_2^{2+} ($X^3\Sigma_g^-$) → CO^+ ($X^2\Sigma^+$) + O^+ (^{4}S) in collinear geometry is in good agreement with the reported experimental dissociation thresholds (with respect to the appearance energy of CO_2^{2+}) of 1.4 ± 0.5 eV [3] or 1.6 ± 0.3 eV.[4] The asymptotic limit of CO^+ ($X^2\Sigma^+$) + O^+ (^{4}S) is computed to be −4.9 eV (computed at $r_1 = 100a_0$ and $r_2 = r_e = 2.255a_0$) with respect to the local minimum, which is close to the reported value of −5.12 eV.

B. Time-Dependent Quantum Mechanical Methodology. The Hamiltonian[19] for a triatomic system with total angular momentum $J = 0$ in the body-fixed (BF) frame is given by

$$\hat{H} = \frac{1}{2}\left[\frac{P_R^2}{\mu_R} + \frac{P_r^2}{\mu_r}\right] + \frac{\mathbf{j}^2}{2I} + V(R, r, \gamma) = -\frac{\hbar^2}{2}\left[\frac{1}{\mu_R}\frac{\partial^2}{\partial R^2} + \frac{1}{\mu_r}\frac{\partial^2}{\partial r^2}\right] - \frac{\hbar^2}{2I}\frac{1}{\sin\gamma}\frac{\partial}{\partial\gamma}\left(\sin\gamma\frac{\partial}{\partial\gamma}\right) + V(R, r, \gamma) \quad (8)$$

where P_R and P_r are the momentum operators corresponding to the two Jacobi distances R and r, respectively, and γ is the angle between R and r. $\mathbf{j}$ is the rotational angular momentum operator for *BC* (CO^+), μ_r is the *BC* (CO^+) reduced mass,

TABLE 1: Parameters of the CO_2^{2+} PES, in Atomic Units

two-body terms $V^{(2)}_{CO+}$

α	$0.1142932E+01$
β	$0.1750739E+01$
c_0	$0.410728820304E+03$
c_1	$-.289715329019E+03$
c_2	$0.165071887420E+03$
c_3	$-.324614464025E+05$
c_4	$0.279487822993E+06$
c_5	$-.112418522213E+07$

two-body terms $V^{(2)}_{OO+}$

α	$0.2173958E+01$
β	$0.8966663E+00$
c_0	$0.493035466706E+02$
c_1	$0.104294278536E+01$
c_2	$-.249869888553E+02$
c_3	$0.212873912440E+03$
c_4	$-.111436121082E+04$
c_5	$0.310214624960E+04$
c_6	$-.452638043349E+04$
c_7	$0.257894737628E+04$

three-body terms $V^{(3)}_{OCO^{2+}}$ for $M=6$

$\beta_{CO}=0.1500001000000000E+01$				$\beta_{OO}=0.5000000000000000E+00$			
i	j	k	d_{ijk}	i	j	k	d_{ijk}
1	1	0	$0.1589622515934708E+03$	0	3	2	$-.1258608503074651E+05$
1	0	1	$-.9487760413336098E+03$	4	1	0	$0.1211541439810606E+06$
1	1	1	$0.3233059503294452E+04$	4	0	1	$-.1372779147718423E+07$
2	1	0	$-.2691343239084217E+04$	0	4	1	$0.3118795276605828E+03$
2	0	1	$0.2405578538441183E+05$	2	2	2	$-.1877196288994309E+07$
0	2	1	$-.6005871930095411E+03$	3	2	1	$-.1840793590480403E+07$
2	1	1	$-.1225662244757521E+06$	3	1	2	$0.7627986898691313E+07$
1	2	1	$-.5284143722906011E+04$	1	3	2	$0.2516779819198058E+06$
2	2	0	$0.9572105240973873E+04$	3	3	0	$0.2445744639144238E+05$
2	0	2	$0.3074082794141343E+06$	3	0	3	$-.8234589674279887E+07$
3	1	0	$0.7220505426688071E+04$	4	1	1	$0.2544265705533639E+07$
3	0	1	$-.3362391640111666E+05$	1	4	1	$-.2528678326262789E+05$
0	3	1	$0.8117290124604615E+03$	4	2	0	$0.7902792810949482E+05$
2	2	1	$.7133153937584469E+05$	4	0	2	$-.1018184998681326E+08$
2	1	2	$-.7321305516588860E+06$	0	4	2	$0.8316655108058862E+04$
3	1	1	$0.7874605492293793E+06$	5	1	0	$-.6380289238486884E+06$
1	3	1	$0.1872861364287135E+05$	5	0	1	$0.2443937600574739E+07$
3	2	0	$-.4861610500628970E+05$	0	5	1	$-.1422022764688491E+04$
3	0	2	$-.9035438814173218E+05$				

TABLE 2: Comparison of the Characteristics of the Fitted PES with the Previously Reported Data

	reported data	present calculations
equilibrium bond length/a_0	2.28[a]	2.26
equilibrium energy/hartree	−186.97847[a]	−186.9805
barrier height with respect to local minimum/eV	1.4 ± 0.5[b], 1.6 ± 0.3[c]	2.0
position of barrier height/a_0	3.61[a]	3.80
asymptote CO^+ ($X^2\Sigma^+$) + O^+ (^4S) energy/eV	−5.12[a]	−4.90

[a] Reference 7. [b] Reference 3. [c] Reference 4.

μ_R [$= m_O(m_{(CO)} + m_O)/(m_O + m_C + m_O)$] is the ($O^+$, CO^+) reduced mass, and I is the moment of inertia of the system defined as $1/I = 1/(\mu_R R^2) + 1/(\mu_r r^2)$. The BF z axis is taken to be parallel to R, and BC lies in the xz plane. $V(R, r, \gamma)$ is the three-body interaction potential.

B.1. Generation of Initial Wave Function. The initial wave function required for the dynamics of CO_2^{2+} is the vibrational wave function for the ground state of neutral CO_2 in its ground electronic state. It was generated using the spectral quantization[20] method using the PES for CO_2 published by Hochlaf et al.[7] For computing the bound-state eigenfunction, a 64 × 64 × 29 grid in (R, r, γ) space was used. A Gaussian function centered at ($R_0 = 3.50\ a_0$, $r_0 = 2.2\ a_0$, $\gamma = 0.212754$ rad) with width parameters $\sigma_R = 0.30\ a_0$, $\sigma_r = 0.25\ a_0$, and $\sigma_\gamma = 0.20$ rad was used as the initial wave packet, and it was propagated on the PES for CO_2 for a total of 7.06 ps. The wave function $\Psi(t)$ at time t is obtained by time evolving the wave packet using the split-operator algorithm[21] for a large number (N_T) of small time-steps (Δt) as

$$\exp\frac{-i\hat{H}\Delta t}{\hbar} = \exp\frac{-iV\Delta t}{2\hbar}\exp\frac{-ij^2\Delta t}{4I\hbar}\exp\frac{-iT\Delta t}{\hbar}\exp\frac{-ij^2\Delta t}{4I\hbar}\exp\frac{-iV\Delta t}{2\hbar} + O(\Delta t^3) \quad (9)$$

where $T = (P_R^2/2\mu_R + P_r^2/2\mu_r)$ is the total radial kinetic energy operator. The action of the exponential operator in T is carried out using the fast Fourier transform algorithm.[21,22] To evaluate the exponential involving the rotational kinetic energy operator,

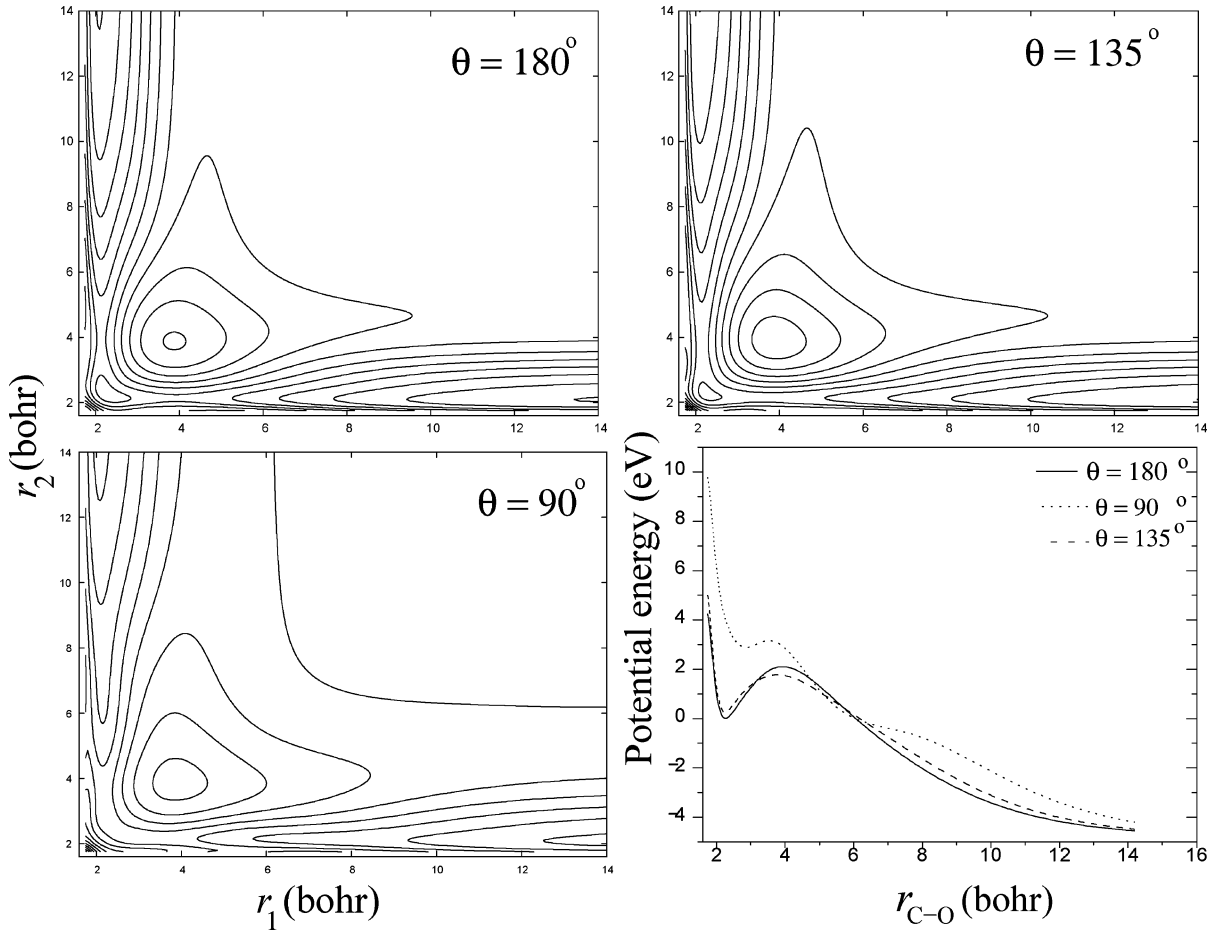

Figure 2. Potential energy contour diagrams (with successive contours differing by 0.05 hartree) for the ground electronic state of CO_2^{++} in (r_1, r_2) space for different values of θ indicated in the panel. Potential energy profiles for the dissociation of CO_2^{2+} are shown for different θ values, with the zero of energy corresponding to the (local) minimum energy geometry of CO_2^{2+}.

TABLE 3: Parameters Used for the Grid and Initial Conditions

parameters	values	remarks
$(R_{min},R_{max})/a_0$	(2.7,6.54)	range of the grid along R
$\Delta R/a_0$	0.06	grid spacing along R
N_R	64	number of grid points along R
$(r_{min},r_{max})/a_0$	(1.725,5.565)	range of the grid along r
$\Delta r/a_0$	0.06	grid spacing along r
N_r	64	number of grid points along r
N_γ	29	number of grid points in γ
$(R_{mask},r_{mask})/a_0$	(4.74,3.765)	starting point of the masking function along (R,r)
Δt/fs	0.2419	length of the time-step used in the propagation
T/ps	7.06	total propagation time

$\exp[-i(\mathbf{j}^2\Delta t)/(4I\hbar)]$, the discrete variable representation[23,24] was used, along with the Gauss−Legendre quadrature.[25]

The eigenvalue spectrum $I(E)$ is obtained by Fourier transforming the autocorrelation function $C(t) = \langle\Psi(0)|\Psi(t)\rangle$:

$$I(E) \propto |\int_0^\infty C(t) \exp\frac{iEt}{\hbar}dt| \quad (10)$$

The eigenfunction for a particular eigenstate is computed by Fourier transforming $\Psi(t)$:

$$\Psi_n = \int_{-\infty}^{\infty} \Psi(t) \exp\frac{iE_nt}{\hbar}dt \quad (11)$$

To avoid numerical errors arising from the reflection or wrap-around of the time-evolved wave packet from the grid edges, the time-evolved wave packet was multiplied by a damping function[26,27] after each time-step of propagation. In the present calculation, the damping function

$$f(X_i) = \sin\left[\frac{\pi}{2}\frac{(X_{mask} + \Delta X_{mask} - X_i)}{\Delta X_{mask}}\right], X_i \geq X_{mask} \quad (12)$$

was used in the asymptotic R and r channels. $X_{mask}(X = R,r)$ is the point at which the damping function was initiated, and $\Delta X_{mask}(= X_{max} - X_{mask})$ is the width of X over which the function decays from 1 to 0, with X_{max} being the maximum value of X in that direction, in a particular channel.

The lowest vibrational state (0, 0, 0) of CO_2 was found to have an energy of 0.315664 eV, in excellent agreement with the reported value of 0.314453 eV,[28] and the next higher energy bound state corresponding to the (1,0,0) state occurs at 0.48226 eV, also in agreement with experimental data.

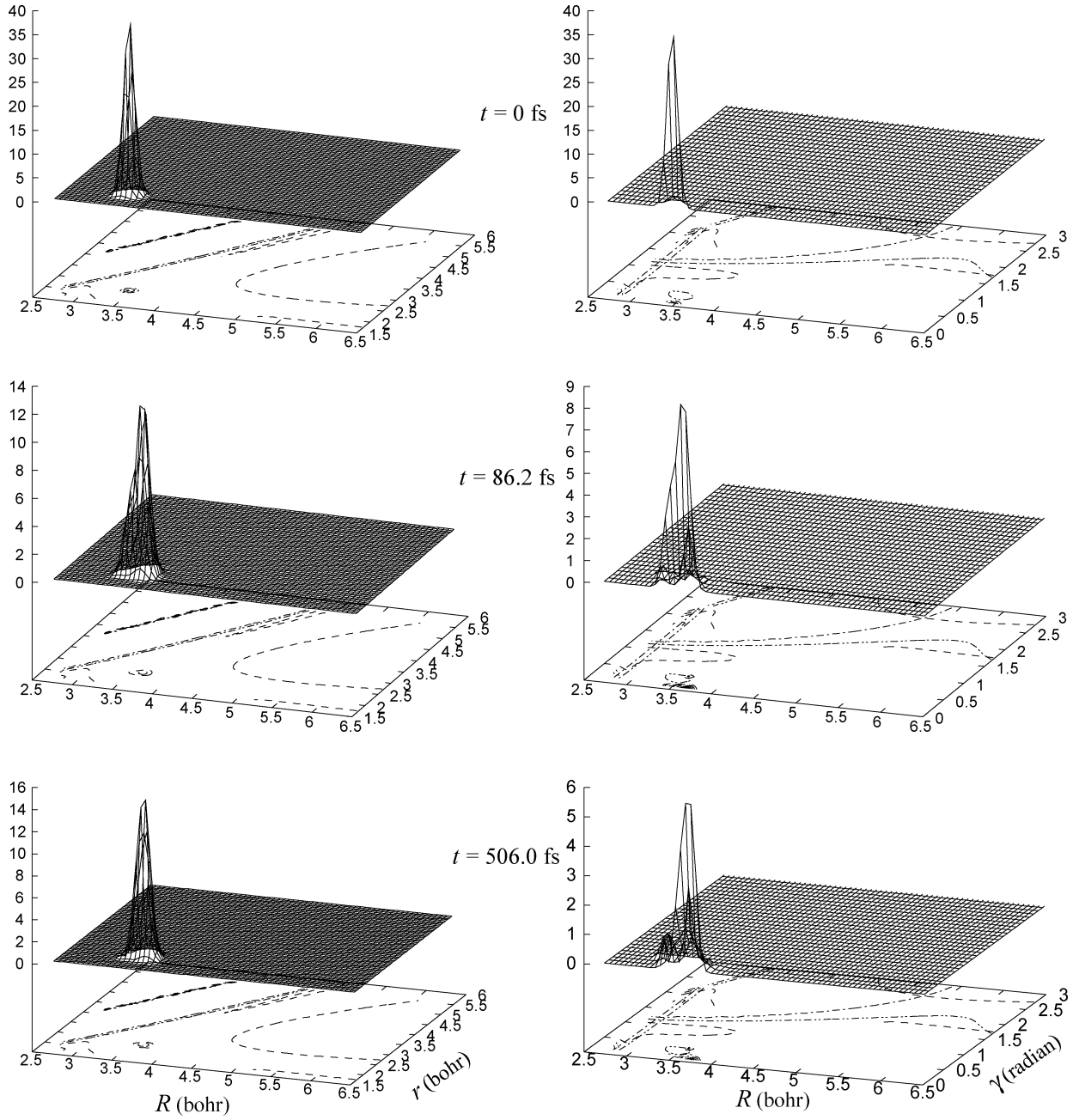

Figure 3. 3D perspective diagram of the probability density and its contours, superimposed on potential energy contours at different intervals of time during the evolution of the wave packet on the ground-state PES of CO_2^{2+}.

B.2. Dissociation Dynamics of CO_2^{2+}. The computed eigenfunction for the ground vibrational state of CO_2 was used as the initial wave function (Condon approximation) for the time-dependent wave packet study on the PES for CO_2^{2+}. The parameters used for the dynamics of CO_2^{2+} dissociation are listed in Table 3. The time evolution of the wave function was carried out for a total of 32 768 time-steps with each step being $\delta t = 0.2155$ fs. The three-dimensional (3D) perspective diagram of the probability density for nuclear motion is shown at different time intervals during the propagation of the wave packet in Figure 3. The computed autocorrelation function is plotted in Figure 4a. Although it decays to ~0.1 in a fraction of a picosecond, it does not decay to zero until 7.06 ps, indicating that there are states with lifetimes greater than 7 ps. Fourier transform of $C(t)$ yields the excitation spectrum plotted in Figure 4b. A Gaussian function having the same half-width (170 meV) as the instrumental resolution function was used for convolving the excitation spectrum to obtain the KER distribution curve plotted in Figure 5. A comparison with the experimental results shows that the computed spectrum is in very good agreement with the experimental result, at low energies. The structures in the predicted spectrum are indicative of the quasibound states supported by the local minimum in the PES of CO_2^{2+}. Further studies are in progress to estimate the lifetimes of these quasibound states. Clear differences between the two spectra at higher energies must be due to the neglect of the excited electronic states of CO_2^{2+} in our study.

IV. Summary and Conclusion

The ab initio ground-state PES has been computed for the CO_2^{2+} system using the MRCI approach with the cc-pVQZ basis set. The PES has a barrier height of 2.0 eV in its equilibrium geometry, with an asymptotic limit of −4.9 eV along the $CO^+(X^2\Sigma^+) + O^+(^4S)$ fragmentation channel. The barrier

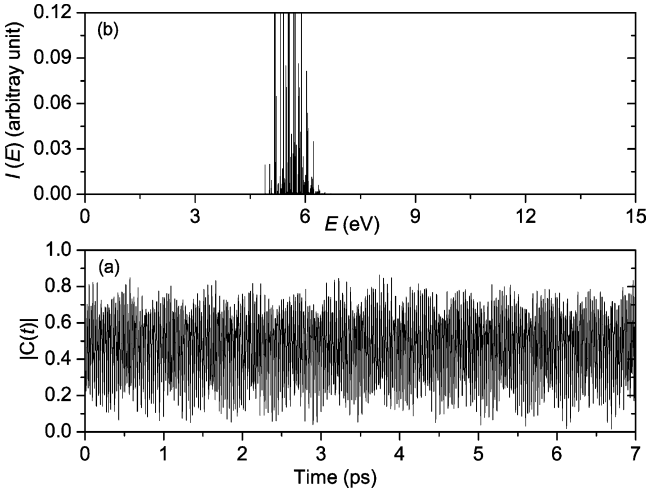

Figure 4. (a) Autocorrelation function for the time evolution on the ground electronic PES of CO_2^{++} and (b) excitation function for the ground electronic state of CO_2^{++}, with the zero of energy corresponding to the (local) minimum energy geometry of CO_2^{++}.

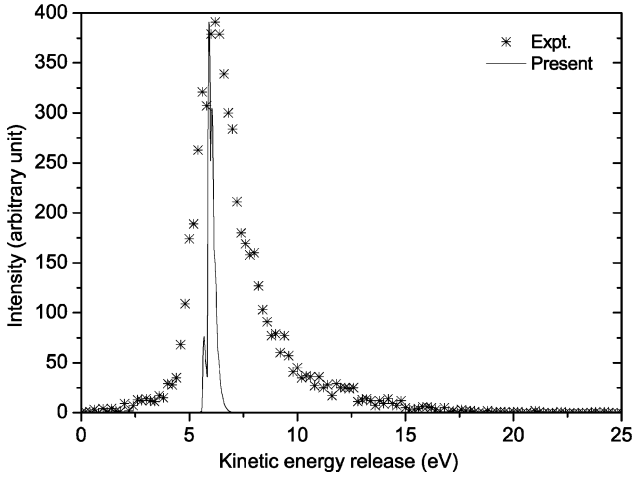

Figure 5. Comparison of the computed KER spectrum for the CO^+ $(X^2\Sigma^+) + O^+ (^4S)$ fragmentation channel with the experimental results obtained by the electron impact ionization of neutral CO_2.

height decreases with decrease in the O−C−O bond angle. Dissociation dynamics of the dication on the computed PES has been studied using the time-dependent quantum mechanical approach, and the excitation spectrum has been calculated. The convoluted excitation spectrum is shown to be in good agreement with the experimental result in the low-energy region. The structures in the predicted spectrum are attributed to the metastable states of CO_2^{2+}. The discrepancy between theory and experiment at higher energies arises presumably due to the noninclusion of the excited states of CO_2^{2+} in the dynamical study.

Acknowledgment. Part of the work reported in this paper was carried out towards the Masters Thesis submitted to IIT Kanpur by J.M. K.G. is grateful to the Council of Scientific and Industrial Research (CSIR), New Delhi, for a fellowship. This study was supported in part by a grant from CSIR, New Delhi. N.S. would like to thank the Department of Science and Technology, New Delhi, for a J. C. Bose fellowship.

References and Notes

(1) Dormann, F. H.; Morrison, J. D. *J. Chem. Phys.* **1964**, *35*, 575.
(2) Märk, T. D.; Hille, E. *J. Chem. Phys.* **1978**, *69*, 2492.
(3) Millie, P.; Nenner, I.; Archirel, P.; Lablanquie, P.; Fournier, P.; Eland, J. H. D. *J. Chem. Phys.* **1986**, *84*, 1259.
(4) Masuoka, T. *Phys. Rev. A* **1994**, *50*, 3886.
(5) Kelber, J. A.; Jennison, D. R.; Rye, R. R. *J. Chem. Phys.* **1981**, *75*, 652. Ågren, H. *J. Chem. Phys.* **1981**, *75*, 1267. Laramore, G. E. *Phys. Rev. A* **1984**, *29*, 23.
(6) Hogreve, H. *J. Phys. B: At. Mol. Opt. Phys.* **1995**, *28*, L263.
(7) Hochlaf, M.; Bennett, F. R.; Chambaud, G.; Rosmus, P. *J. Phys. B: At. Mol. Opt. Phys.* **1998**, *31*, 2163.
(8) Slattery, A. E.; Field, T. A.; Ahmad, M.; Hall, R. I.; Lambourne, J.; Penent, F.; Lablanquie, P.; Eland, J. H. D. *J. Chem. Phys.* **2005**, *122*, 084317.
(9) Balakrishnan. N.; Kalyanaraman, C.; Sathyamurthy, N. *Phys. Rep.* **1997**, *280*, 79.
(10) Krishnamurthy, M.; Gross, P.; Mathur, D. *Rapid Commun. Mass Spectrom.* **1995**, *9*, 358; *Phys. Rev. A* **1994**, *50*, 2383.
(11) Tarisien, M.; Adoui, L.; Frémont, F.; Leliévre, D.; Guillaume, L.; Chesnel, J.-Y.; Zhang, H.; Dubois, A.; Mathur, D.; Kumar, S.; Krishnamurthy, M.; Cassimi, A. *J. Phys. B: At. Mol. Opt. Phys.* **2000**, *33*, L11.
(12) Sharma, V.; Bapat, B. *Eur. Phys. J. D* **2006**, *37*, 223.
(13) Bapat, B.; Sharma, V. *Int. J. Mass Spectrom.* **2006**, *251*, 10.
(14) Field, T. A.; Eland, J. H. D. *Chem. Phys. Lett.* **1993**, *211*, 436.
(15) Newton, A. S.; Sciamanna, A. F. *J. Chem. Phys.* **1964**, *40*, 718.
(16) Tsai, B. P.; Eland, J. H. D. *Int. J. Mass Spectrom. Ion Phys.* **1980**, *36*, 143.
(17) Werner, H.-J.; Knowles, P. J.; Almlöf, J.; Amos, R. D.; Deegan, M. J. O.; Elbert, S. T.; Meyer, W.; Peterson, K.; Pitzer, R.; Stone, A. J.; Taylor, P. R. *MOLPRO*, version 2000.1; University of Birmingham: Birmingham, U.K., 2001.
(18) Aguado, A.; Tablero, C.; Paniagua, M. *Comput. Phys. Commun.* **1998**, *108*, 259.
(19) Zhang, J. Z. H. *Theory and Application of Quantum Molecular Dynamics*; World Scientific: Singapore, 1999.
(20) Feit, M. D.; Fleck, J. A., Jr.; Steiger, A. *J. Comput. Phys.* **1982**, *14*, 368.
(21) Fleck, J. A., Jr.; Morris, J. R.; Feit, M. D. *Appl. Phys.* **1976**, *10*, 129.
(22) Kosloff, D.; Kosloff, R. *J. Comput. Phys.* **1983**, *53*, 35.
(23) Lill, J. V.; Parker, G. A.; Light, J. C. *Chem. Phys. Lett.* **1982**, *89*, 483.
(24) Light, J. C.; Hamilton, I. P.; Lill, J. V. *J. Chem. Phys.* **1985**, *82*, 1400.
(25) Press, W. H.; Flannery, D. P.; Teukolsky, S. A.; Vetterling, W. T. *Numerical Recipes: The Art of Scientific Computing*; Cambridge University Press: Cambridge, U.K., 1986.
(26) Bisseling, R. H.; Kosloff, R.; Manz, J. *J. Chem. Phys.* **1985**, *83*, 993.
(27) Mahapatra, S.; Sathyamurthy, N. *J. Chem. Soc., Faraday Trans.* **1987**, *93*, 773.
(28) Herzberg, G. *Electronic Spectra and Electronic Structure of Polyatomic Molecules*; Van Nostrand: New York, 1966.